Modeling Urban Tree Growth for Digital Twins: Transformation of Point Clouds into Parametric Crown Models

Yong Guo[1], Andreas Luka[2], Yunqi Wei[3]

[1]Department of Landscape Architecture, School of Architecture, Tsinghua University/China · guoyong_cn@tsinghua.edu.cn
[2]Next Generation Landscape Architecture Research Center/China · andreas@luka-oline.de
[3]School of Landscape Architecture, Beijing Forestry University/China · weiyunqi2777@gmail.com

Abstract: Digital twins of urban trees require sufficient 3D model and simulation functionality for growth and ecosystem service estimation. To achieve this level of functionality, the author proposed a workflow utilizing terrestrial laser scanning to generate the point clouds of individual trees. Based on the point clouds, by utilizing convex hull and α-hull, shape control parameters were measured and extracted and used to create Cescatti hulls for selected trees' parametric crown models. Tree skeletons were extracted from point clouds and reconstructed into quantitative structure models. Both the crown models and tree skeletons were used to calculate the above-ground biomass of the trees and their sequestered carbon amounts. Allometric equations and procedural algorithms were then applied to simulate and predict the growth and biomass changes. The outcome of the models and the results' prediction and estimation indicated that the proposed workflow was sufficient to offer a promising starting point for achieving the functionality of digital twins.

Keywords: Existing urban tree, digital twins, point clouds, hull model, simulation

1 Introduction

The urban trees' ecosystem services perform an essential role in mitigating the impact of climate change by reducing greenhouse gases as a result of sequestering carbon dioxide, removing pollutants from the air, and reducing stormwater runoff. They also assist in adapting cities to higher temperatures by providing shadowing and cooling in open spaces (RÖTZER 2019) and reducing the amount of energy needed to heat and cool buildings. These roles can be quantified at the scale of individual trees or for entire cities (MCPHERSON et al. 2005). As a result of the increased importance of the urban trees' ecosystem functions and challenges resulting from worsening environmental conditions, accurate geometrical representations, monitoring tree parameters, and predicting growth are important. Suitable geometrical representations support the incorporation of existing trees into modern planning tools (e. g., BIM/LIM and CIM). LiDAR and photogrammetry-based point clouds can identify existing trees in these planning tools with high accuracy but are not suitable for applying simulations. Monitoring tree parameters is essential for estimating ecosystem services. Some of the crucial eco-services are directly linked to parameters, i. e., the wooden components of the above-ground biomass (AGB) are directly connected with carbon sequestration, leaf area with pollutant removal, and leaf area index with shadowing. Simulating growth allows the performance of cost-benefit analysis (MCPHERSON et al. 2010, SUNDERLAND et al. 2012) and the consideration of alternative management scenarios (MCPHERSON et al. 1994).

The growth of urban trees differs significantly from trees of the same species in a forest or natural environment. Higher temperatures in urban areas may lead to faster growth rates

Journal of Digital Landscape Architecture, 7-2022, pp. 213-223. © Wichmann Verlag, VDE VERLAG GMBH · Berlin · Offenbach. ISBN 978-3-87907-724-3, ISSN 2367-4253, e-ISSN 2511-624X, doi:10.14627/537724021.

(PRETZSCH et al. 2017), and broader stands may lead to wider crowns and larger branches (MACFARLANE and KANE 2017). Therefore, forest growth models may be inadequate for predicting the growth of urban trees (MCPHERSON, NOWAK).

A satisfactory 3D model with the capabilities of simulating growth and functions, as well as mechanisms for validation and calibration are required to create a digital twin of a tree (GOBEWAN et al. 2020).

In recent years, significant progress has been made in deriving the tree- and stand-level attributes from terrestrial laser scan (TLS) data to depict forest productivity, evolution, and ecological functions (LIANG et al. 2018). Thus, the wooden part's volume can be measured directly and converted into biomass and sequestered carbon. GOBEWAN et al. (2020) presented a framework using TLS data, extracting the skeleton, and applying L-Systems for growth simulation.

Nevertheless, allometric equations-based estimations are still important tools, especially for trees with leaf conditions or lower density point clouds from photogrammetry or aerial laser scans. TAO et al. (2014) demonstrated that the above-ground biomass (AGB) can be estimated using crown volumes derived from point clouds.

Repeated high-accuracy TLS over several years can improve allometric equations as well as validating and calibrating growth predictions.

Our work shows a complete workflow that can be automated for model trees based on TLS, extract skeletons and predict their further growth based on species-level growth equations as well as a more cost-effective approach with photogrammetry-based point clouds, estimated the diameter at the breast height (DBH), height and crown volume and their allometric relationships as well as a framework for continual improvement.

2 The Reconstruction of the Geometrical Model of the Existing Trees

2.1 Subject: Scholar Trees on University Campuses

The Scholar tree (*Sophora japonica*) is an indigenous deciduous broad-leaved tree in Northern China. It has pinnate compound leaves with 7-15 leaflets and panicle flowers in yellow and white, as well as fleshy undivided beaded pods. It blooms from July to August and fruits from August to October. It is distributed across numerous provinces in both north and south China. It can also be found in Japan, Vietnam, Korea and many European and American countries.

The adult tree typically reaches a height of 25 meters. In Beijing, people incorporated 500 years old scholar trees in traditional courtyard areas. Owing to its longevity, superior adaptability, broad shading canopy and beautiful shape, it has been well accepted and has been planted as an urban greening tree in large numbers. For example, in the 2 central districts in Beijing city, the quantity of scholar trees accounts for 57.4% of the total number of urban trees, which makes it a typical urban tree species.

The research subjects were selected scholar trees standing in one of the university campuses in Beijing. Beijing has a warm temperate semi-humid continental monsoon climate, hot and rainy in summer, cold and dry in winter, with short spring and autumn seasons, with an average annual temperature of 10-12 degrees Celsius, mean annual precipitation is about 600mm, with 190-195 frost-free days.

The subject group of 40 scholar trees stands on both sides of the central lawn in two rows. The ages of the selected trees range from 8 to 150 years. Some of them were newly planted 2 years ago to replace the dead ones after a disease. Some of them were heavily pruned with their main branches missing and partial crown. 19 trees have kept their full crown and complete branches and a natural growing shape. This variation is typical of the complexity of existing urban trees.

2.2 Data Input: Point Cloud Treatment

The site was scanned twice – in November 2020 and April 2021. This generated 2 data-sets of point clouds. In between the scans was the trees' dormant period, thus the changes that the two sets of data described only relate to leaves and crowns. The first set of data was derived from FARO focus plus S70 and represented scholar trees' autumn shape with most of the leaves. The second set of data was derived from Leica BLK 360 and represented the early spring situation with no leaves.

The FARO point cloud was derived from 85 scanning positions with the position registration accuracy being 12.22 mm, and 780 million points were included. The Leica point cloud was derived from 118 positions containing 496 million points with an accuracy of 5 mm and covered a larger area, which included the facades of the surrounding buildings. For both sets of data information, the x, y, z of the points, R, G, B values of the color, as well as directions of vectors were extracted (Figure 1).

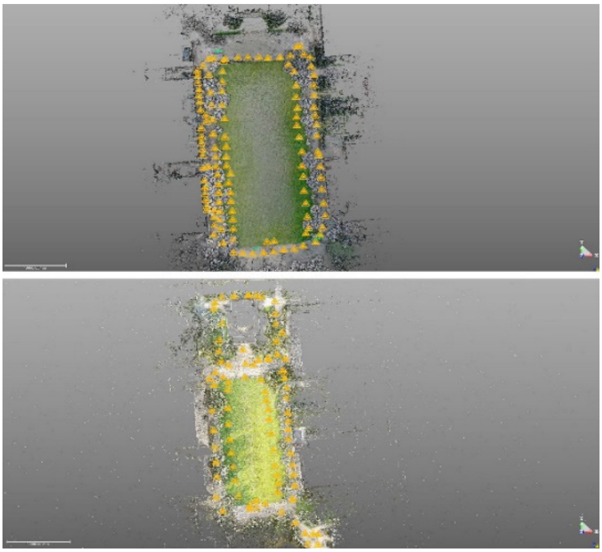

Fig. 1:
TLS positions of the 2 sets of point clouds

After the registration, 2 sets of complete data were obtained with GIS locations to describe the integrated environment. The data was subsequently processed by utilizing de-noise and segmentation. The point cloud of individual trees was produced and the crown and skeleton were subsequently separated.

2.3 The Key Method: Reconstruction of the Tree Components

Height and DBH measurement

The DBH and height in the field were measured, and their values from both point clouds were extracted. The height was extracted from the highest point of the de-noised and segmented point clouds. The diameter at the breast height (DBH) was calculated from a fitted cylinder at the height of 1.37m in the software CompuTree. The field-measured values and extracted values were analyzed by utilizing linear regression analysis to find potential bias.

Crown Volume and Surfaces Extraction

The crown volume included the entire living canopy of the tree from the base to the upper edge of the living crown, which was also approximately represented by the outer edge of the branch tips inward. It does not include dead branches above or below the living portion of the canopy, nor any epicormic sprout below the base of the living crown. It may include hollows or voids encompassed within those boundaries.

By combining color and spatial distance filters, the crown volume was derived as the subset of specific points related to leaves from non-epicormic sprouts.

The optimal approximation of the crown volume and surface with their convex hull and the smallest convex shape that included all points was produced. Convex hulls are not able to represent gaps and voids. Hulls were applied based on α-shapes, a closed polyhedron determined uniquely by the point set and the parameter α, controlling the level of detail of the polyhedron. The hulls were created with MeshLab (open-source software), and Python for better integration into the workflow.

From the α-shape, asymmetric CESCATTI hulls (1997) were constructed. The envelope was defined using six control points (top and base points of the crown and four other points representing the largest radius in two orthogonal directions) and two from parameters controlling its convexity.

The two form parameters are unique to the species and were derived by analysis of images from undisturbed grown existing crowns. A python script was constructed to extract the six points from the α-shape hull.

Tree Skeleton Extraction

By applying the software and plugin CompuTree/SimpleForest, the skeleton was extracted as point clouds, meshes, and cylinders using the quantitative structure model (QSM). From the set of hierarchically structured cylinders fitted to the trunk (stem) and branches, the specific volume for each tree's trunk and branches was calculated. The results were verified by running several analyses in the software R.

To understand the impact of the massive pruning during replanting, the trees were grouped by corresponding analysis on the distribution of branch sizes and the results were compared with information from the planting and replanting schedule.

3 Simulation for Digital Twin Functionality

3.1 Biomass Estimation

The above-ground biomass (AGB) was estimated for each tree by allometric equation from the DBH and the height by utilizing the following two equations:

$$w = 0.093(D^2H)^{0.869} \quad (1)$$

$$w = 0.116(D)^{2.307} \quad (2)$$

In these equations, *w* stands for AGB in kg, *D* is the DBH in cm, *H* is the height of the tree in metres.

The underground biomass was estimated based on the average reference value of the tree rhizome ratio of broadleaved forests, which was proposed by the 2006 Intergovernmental Panel on Climate Change, IPCC.

3.2 Sequestered Carbon Estimation

The sequestered carbon was estimated based on the estimated AGB's by using the following equations:

$$C = \sum_{i=1}^{n}(WI_{i\,above} + W_{i\,under}) \bullet CF_i \quad (3)$$

In this equation, *C* is the carbon stock of the tree level; *i* stands for different tree species; n is the total number of species; W_i above is the AGB of the specific species *i*; $W_{i\ \mathrm{under}}$ is the underground biomass of the specific species *i*; CF_i is the carbon content rate of the tree species *i*. In Beijing the carbon content rate is 0.502.

3.3 Further Growth Prediction

We predicted further growth for the DBH/hulls utilizing empirical models.

The model for the growth of height, spread, the height of largest crown radius, and stem height is the three-parameter Chapman-Richards growth equation:

$$\mathrm{y(t)} = \mathrm{A}(1 - \mathrm{e}^{-\mathrm{kt}})^{\mathrm{p}} \quad (4)$$

and the model for the growth of DBH is the four-parameter Richard equation:

$$\mathrm{y(t)} = \mathrm{A}(1 - \mathrm{Se}^{-\mathrm{kt}})^{\mathrm{p}} \quad (5)$$

A is the upper asymptote of the curve, k controls the slope at the inflection point, and p controls the relative size at the inflection point.

The first model has its starting point at the origin of the axis, which is only useful if growth starts at zero. For the second model, S determines the horizontal shift of the curve. The parameter S, k, and p can have no direct biological interpretation. These models can be reparametrized with meaningful interpretable growth parameters (TJØRVE & TJØRVE 2010, LUKA 2022).

To project the future size and form of the hulls, we computed and applied transformation vectors for each hull defining point based on its position and the growth model.

4 Results: Digital Twins of Existing Urban Trees

4.1 The Workflow of Digital Twin Trees

The experiment verified the proposed workflow. By applying several software packages in sequence, point clouds of the selected urban trees were calculated and parametric geometrical models were reconstructed accordingly. By fitting the parameters to allometric equations, it was possible to simulate the growing of tree crowns and the increase in biomass. These parameters are related to the estimation of current and future sequestered carbon amounts. The outcome of the workflow included not only the geometrical model but also the simulation functionality. It demonstrated the variety and complexity of the current situation relating to existing trees and predicted their future growth and development, which fulfilled the basic function of a digital twin (Figure 2).

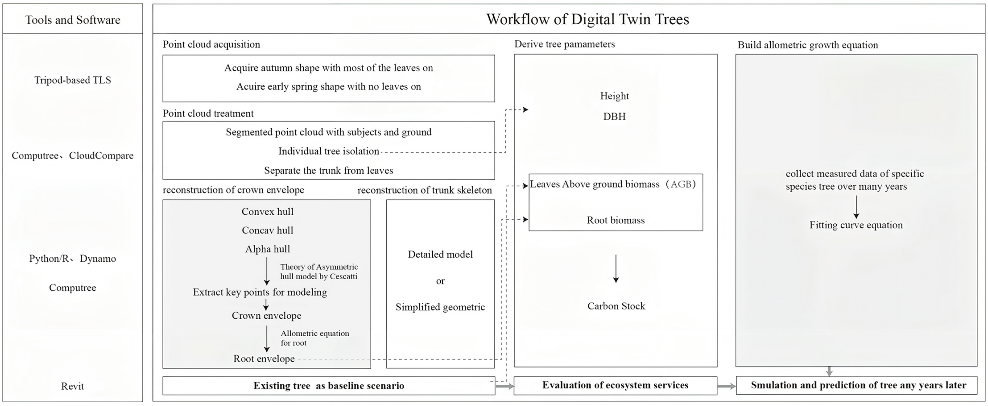

Fig. 2: Diagram of the workflow of digital trees

4.2 The Outcome of Modeling: Real-Time TLS for Parametric Hulls and Skeletons

As the experimental workflow proceeded, a series of models were produced, including the point cloud derived from TLS as a real-time data source (Figure 3), the de-noised and segmented point clouds of groups and individual trees as data input for parametrical reconstruction (Figure 4-5), as well as the subgroups of points that represented tree crowns and skeletons separately These are the necessary partial models for increasing the accuracy and efficiency of the subsequent computation.

Fig. 3: Point cloud of the existing trees on campus deriving from TLS

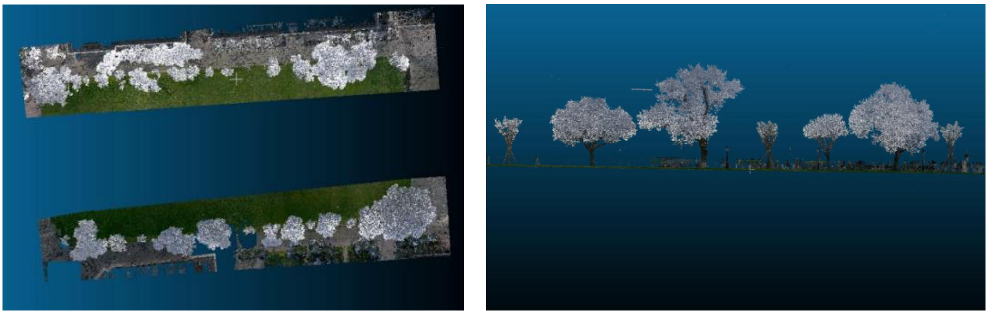

Fig. 4: Segmented point cloud with subjects and ground

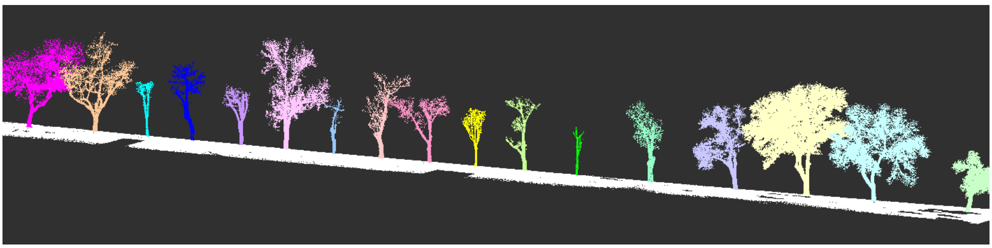

Fig. 5: The clear up point cloud of single trees

The point clouds were transformed into parametric geometrical models by processing the data in the forms of convex hull, concave hull and α-hull. Parameters that perform the shape-controlling function were extracted from the hulls and used to create the Cescatti hull of the tree crowns (Figure 6-7). The Cescatti hull is the starting point for the subsequent growing simulation of the crown volume.

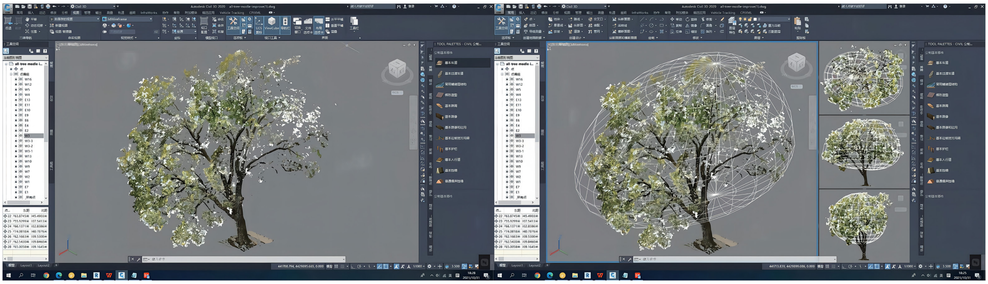

Fig. 6: Isolated point clouds of the selected tree and its Cescatti hull model as crown envelope

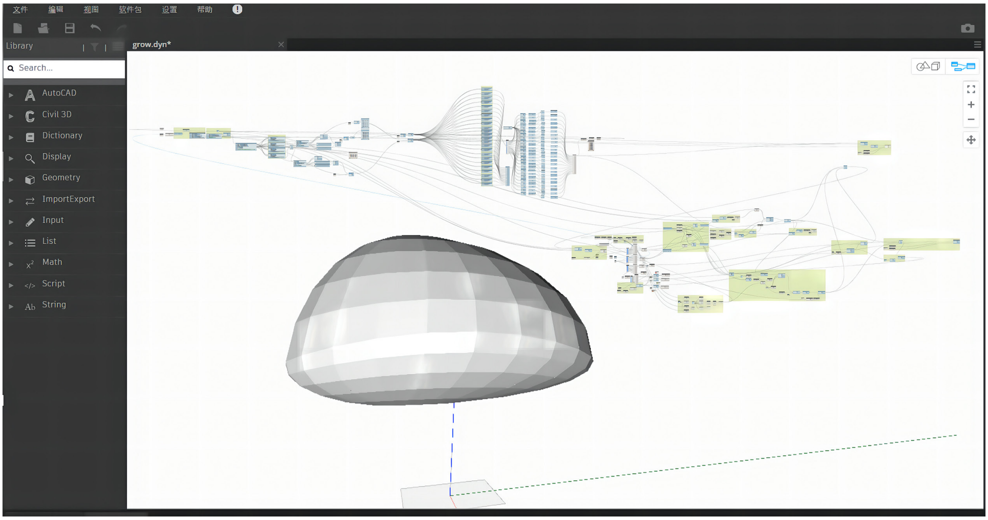

Fig. 7: Dynamo script to parametrically generate the tree crowns

The trunks and branches of the tree were accurately modeled by utilizing the quantitative structure model. The outcome of the modeling demonstrated numerous details and reflected the actual spatial feature of the tree (Figure 8). The detailed skeleton was not only a representation of the tree but also the starting point for calculating the quantity of the wooden parts in order to estimate the above-ground biomass.

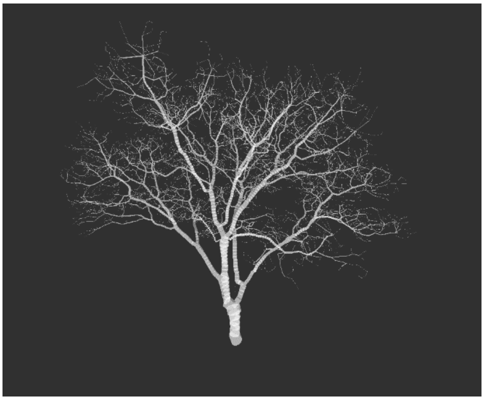

Fig. 8:
Quantitative structure model of tree skeleton extracted from point cloud

The outcome also included the Revit model by integration into the BIM/LIM/CIM environment (Figure 9).

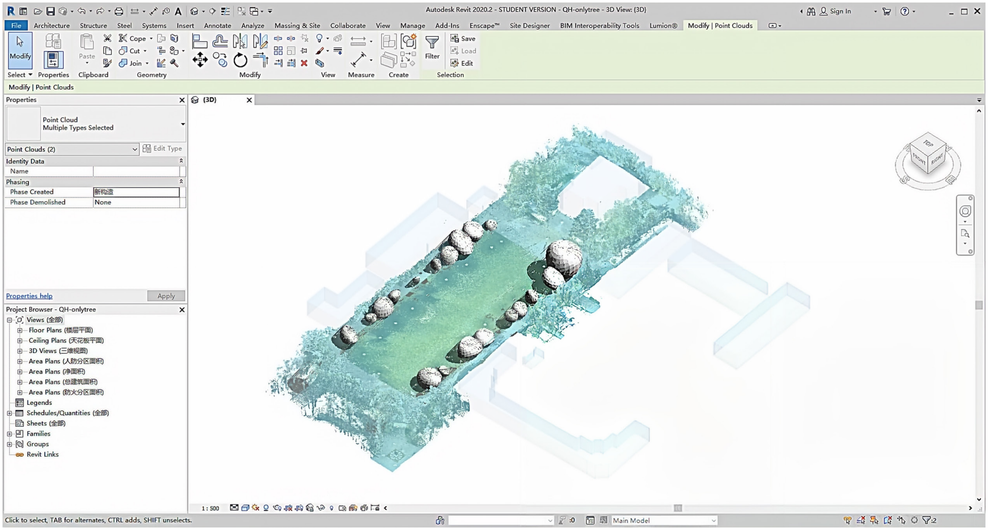

Fig. 9: Point clouds of trees are replaced by the reconstructed LIM tress in Revit

4.3 Simulation and Prediction of Ecosystem Service

19 trees were selected, all of which had complete tree crowns and non-pruned main branches, to run the growth simulation by utilizing proposed growth simulation formulae. The results of the simulation demonstrated that the gross biomass of the selected trees will reach 20124.21 kg in 10 years, 34226.42 kg kg in 50 years, and the gross carbon stock will increase to 10102.35 kg in 10 years and to 17181.66 kg in 50 years.

Table 1: Growth simulation results of trees

Sampling number	Tree height/ m	Current		Ten years later		Twenty years later		Thirty years later		Forty years later		Fifty years later	
		Biomass/ kg	Carbon stock/ kg	Biomass/ kg	Carbon stock/ kg	Biomass/ kg	Carbon stock/ kg	Biomass/ kg	Carbon stock/ kg	Biomass/ kg	Carbon stock/ kg	Biomass/ kg	Carbon stock/ kg
E2	1458.12	1643.12	1809.43	908.33	1965.42	986.64	2110.53	1059.49	2245.22	1127.10	2368.58	1189.03	1458.12
E4	1129.29	566.90	1320.64	662.96	1503.56	754.79	1676.95	841.83	1841.38	924.37	1995.05	1001.52	1129.29
E6	312.34	156.79	464.93	233.39	640.69	321.63	827.06	415.19	1018.09	511.08	1208.37	606.60	312.34
E7	1302.59	653.90	1485.18	745.56	1660.26	833.45	1825.68	916.49	1980.52	994.22	2124.86	1066.68	1302.59
E9	583.22	292.78	770.53	386.80	960.85	482.35	1151.85	578.23	1339.35	672.36	1521.00	763.54	583.22
E10	1082.87	543.60	1264.99	635.03	1449.37	727.58	1626.09	816.30	1793.19	900.18	1950.40	979.10	1082.87
E11	230.30	115.61	383.51	192.52	551.00	276.60	733.22	368.08	922.59	463.14	1113.71	559.08	230.30
E12	221.68	111.29	367.86	184.67	533.37	267.75	714.37	358.61	903.25	453.43	1094.30	549.34	221.68
E13	678.09	340.40	864.87	434.16	1056.45	530.34	1245.95	625.47	1431.37	718.55	1608.57	807.50	678.09
W1	645.87	324.22	827.06	415.19	1018.09	511.08	1208.37	606.60	1394.75	700.16	1573.85	790.07	645.87
W2	1045.50	524.84	1227.59	616.25	1413.03	709.34	1591.15	798.76	1760.47	883.76	1919.89	963.78	1045.50
W3	1215.36	610.11	1394.75	700.16	1573.85	790.07	1744.55	875.76	1903.81	955.71	2053.65	1030.93	1215.36
W4	992.44	498.20	1189.83	597.29	1376.14	690.82	1556.14	781.18	1727.54	867.23	1888.40	947.98	992.44
W5	1047.82	526.01	1245.95	625.47	1431.37	718.55	1608.57	807.50	1777.10	892.11	1935.44	971.59	1047.82
W7	641.39	321.98	827.06	415.19	1018.09	511.08	1208.37	606.60	1394.75	700.16	1573.85	790.07	641.39
W9	460.70	231.27	641.39	321.98	827.06	415.19	1018.09	511.08	1208.37	606.60	1394.75	700.16	460.70
W10	769.30	386.19	960.85	482.35	1151.85	578.23	1339.35	672.36	1521.00	763.54	1694.29	850.53	769.30
W12	1125.05	564.77	1320.64	662.96	1503.56	754.79	1676.95	841.83	1841.38	924.37	1995.05	1001.52	1125.05
W13	407.40	204.51	586.61	294.48	770.53	386.80	960.85	482.35	1151.85	578.23	1339.35	672.36	407.40
W16	980.50	492.21	1170.55	587.61	1357.67	681.55	1538.47	772.31	1710.56	858.70	1873.06	940.28	980.50
Average		816.49	455.44	1006.21	505.12	1188.11	596.43	1368.13	686.80	1543.33	774.75	1711.32	859.08
Gross		16329.82	9108.72	20124.21	10102.35	23762.22	11928.64	27362.58	13736.02	30866.54	15495.00	34226.42	17181.66

4.4 Validation

Access the quality of DBH and height derived from TLS, we performed a simple regression analysis against field measured values. The DBH and height measured with TLS was highly correlated (R2 = 90.01) with the values measured in field and free of systematic bias.

We performed pairwise t-test to compare the AGB calculated with the allometric formulas and the AGB based on volume extracted from the TLS. There was a significant difference in the AGB from allometric equations and from TLS with t(19) = –3.8866 and p = 0.005, mean difference = –388.70).

5 Discussion and Outlook: The Optimization of the Workflow

The results indicated that the proposed workflow for modeling urban trees was able to produce adequate 3D models and to achieve the functions of simulating growth and estimating ecosystem functions. Thus, the workflow was adequate to provide a solid starting point in order to achieve the functions of digital twins.

For future practical applications, the workflow will require further optimization. Firstly, it will be necessary to undertake further software development to achieve complete automation. The algorithms for point cloud de-noising, individual tree recognition, and QSM need to be seamlessly integrated with the algorithms for alpha and parametric hull determination. Secondly, it will be necessary to reduce the cost of data harvesting. Therefore, the airborne photogrammetry and the other technologies that will improve the rapid massive scan should be studied and integrated into the workflow.

The currently used allometric equations for AGB produce significant errors when applied to urban trees that have been heavily pruned. The massive pruning also causes significant disturbance to the growth pattern and currently applied growth equations are not accurate when applied to this level of disruption. Further research will be required and allometric models based on hulls should be studied as well as growth modeling using procedural growth on the QSM.

It is also necessary to improve the validation and calibration mechanism to complete the function of digital twin. To verify the prediction and estimation from the results, it is necessary to keep monitoring the subject and measure the growth and services into the future. To obtain a continual capability of monitoring, it is necessary to include the Internet of Things into the subsequent research.

References

CESCATTI, A. (1997), Modelling the radiative transfer in discontinuous canopies of asymmetric crowns. I. Model Structure and algorithms. Ecological Modelling, 101 (2-3), 263-274.

GOBEAWAN, L., LIN, E., TANDON, A. et al. (2018), Modeling Trees for Virtual Singapore: From Data Acquisition to CityGML Models. The International Archives of the Photogrammetry, Remote Sensing and Spatial Information Sciences, XLII-4/W10, 55-62.

LIANG, X., KANKARE, V., HYYPPÄ, J. et al. (2016), Terrestrial laser scanning in forest inventories. ISPRS J Photogramm Remote Sens, 115, 63-77.

LUKA, A. (2021), http://alcbimlab.com/BIM/BIM-7.html (09.12.2021).

MACFARLANE, D. & KANE, B. (2017), Neighbour effects on tree architecture: functional trade-offs balancing crown competitiveness with wind resistance. Functional Ecology, 31 (8), 1624-1636.

MCPHERSON, E. & SIMPSON, J. (2003), Potential energy savings in buildings by an urban tree planting programme in California. Urban Forestry & Urban Greening, 2 (2), 73-86.

MCPHERSON, E., SIMPSON, J., XIAO, Q. & WU, C. (2011), Million trees Los Angeles canopy cover and benefit assessment. Landscape and Urban Planning, 99 (1), 40-50.

PRETZSCH, H., BIBER, P., UHL, E. et al. (2017), Climate change accelerates growth of urban trees in metropolises worldwide. Sci Rep 7, 15403.

RÖTZER, T., RAHMAN, M. A., MOSER-REISCHL, A., PAULEIT, S. & PRETZSCH, H. (2019), Process based simulation of tree growth and ecosystem services of urban trees under present and future climate conditions. Science of The Total Environment, 676, 651-664.

SUNDERLAND, T., ROGERS, K. & COISH, N. (2012), What proportion of the costs of urban trees can be justified by the carbon sequestration and air-quality benefits they provide? Arboricultural Journal, 34 (2), 62-82.

TECHNICAL REGULATIONS FOR FORESTRY CARBON ACCOUNTING AND MONITORING (DB11/T 953) (2013).

TJØRVE, E. & TJØRVE, K. M. C. (2010), A unified approach to the Richards-model family for use in growth analyses: why we need only two model forms [J]. Journal of Theoretical Biology, 267 (3), 417-425.